

Analysis and Design of Concrete Columns for Biaxial Bending—Overview

by Richard W. Furlong, Cheng-Tzu Thomas Hsu, and S. Ali Mirza

Columns with axial load causing biaxial bending are present in many different building structures. The provisions of ACI 318 Section 10.2 are the basis for traditional design aids that show section strength when moments act in a plane of symmetry. Strength analysis for biaxial bending is significantly more difficult, as moments are not applied in a plane of symmetry. Several methods of analyses that use traditional design aids are reviewed and the results are compared with data obtained from physical tests of normal strength concrete columns subjected to short-term axial loads and biaxial bending. Results indicate that any among the four different methods of cross-sectional analysis are equally suitable for design purposes. The value of three-dimensional interaction diagrams in the design process is discussed. Computer-based methods of analysis are also described and compared with test observations.

Keywords: column; reinforced concrete; strength; surface.

INTRODUCTION

Columns resisting axial load and biaxial bending can exist in building structures. Column bending is uniaxial when the axial load acts at an eccentricity along one of the principal axes (in a plane of section symmetry), and column bending is biaxial when the load is applied at an eccentricity that is not along a principal axis. Analysis of a rectangular cross section in uniaxial bending uses an equivalent rectangular stress block acting on a rectangular area of compressed concrete and a neutral axis (axis of zero strain) that is perpendicular to the direction of the eccentricity. Any lateral deflection along the longitudinal axis of the column under uniaxially eccentric compression loads remains in the plane of section symmetry. Analysis of stress on a rectangular cross section in biaxial bending can involve a triangular or trapezoidal area of compressed concrete, as well as a neutral axis that is not perpendicular to the direction of the eccentricity. Generally, the lateral deflection along the longitudinal axis of the column under biaxially eccentric compression loads is in a direction different from the direction of the eccentricity.

Cross sections under service load conditions with low levels of compressive stress and no cracking of concrete have a unique geometric centroid that can be determined with elastic analysis methods of solid mechanics after steel areas are transformed by the modular ratio (E_s/E_c) between steel and concrete. Because concrete cracks at low tensile stress, it does not effectively resist tension, and any area of tensile concrete is neglected. Consequently, in the presence of tensile strain, the portion of the cross section in compression varies with load and eccentricity. The elastic analysis of transformed rectangular cross sections under uniaxially eccentric compression remains relatively simple because equilibrium equations yield a second-order polynomial for locating the neutral axis.¹ Under biaxially eccentric compression, the equilibrium equations can be solved iteratively. After the location and

angular orientation of the neutral axis have been established, displacements and concrete and steel stresses can be estimated for service load conditions.

Cross sections in which material stress is not proportional to material strain are more complex to analyze because the elastic superposition of stresses does not apply. Methods of analysis for such cross sections are described herein. Strength design must be based on the cross section ultimate strength, which is not influenced by the sequence of load that causes failure. Several design procedures for ultimate strength analysis are examined in this paper and recommendations for design are offered. The results of the study are limited to normal-strength concrete columns subjected to short-term loads.

RESEARCH SIGNIFICANCE

Reinforced concrete columns can be subjected to combined biaxial bending moments and axial load. Current building codes, however, do not give enough guidelines for the design and analysis of these structural elements. This study presents an overview of recently developed design and computer analysis methods, and they are compared with many short and slender columns under actual tests. Examples are also provided for engineering practices.

ANALYSIS PROCEDURES FOR STRENGTH INTERACTION SURFACES

Several writers on the analysis of the ultimate strength of biaxially loaded columns explained the relationships that are needed to consider nonlinear stress distributions throughout a plane strain field.²⁻⁴ An equivalent compression zone, similar to the one developed by Whitney⁵ and given in ACI 318 Section 10.2.7,⁶ was used to model concrete in the compression zone for calculating ultimate strength. ACI 318⁶ Section 10.2.3 specifies the maximum usable concrete strain to be 0.003. That strain together with any location and orientation of a neutral axis defines failure condition for which one set of failure coordinates P_n , M_{nx} , and M_{ny} can be evaluated. The locus of all such points is a strength interaction surface. One quadrant of such a graph is shown in Fig. 1. Moment contours representing planes of constant axial load have been used to describe the three-dimensional ultimate strength interaction diagram (Fig. 1). These contours are similar to a series of ellipses for reinforced concrete rectangular cross sections.^{7,8}

ACI Structural Journal, V. 101, No. 3, May-June 2004.

MS No. 03-120 received March 10, 2003, and reviewed under Institute publication policies. Copyright © 2004, American Concrete Institute. All rights reserved, including the making of copies unless permission is obtained from the copyright proprietors. Pertinent discussion including author's closure, if any, will be published in the March-April 2005 *ACI Structural Journal* if the discussion is received by November 1, 2004.

Richard W. Furlong, *FACI*, is a professor emeritus at the University of Texas, Austin, Tex. He is a member of ACI Committees 335, Composite and Hybrid Structures; 340, Design Aids for ACI Building Codes; and Joint ACI-ASCE Committee 441, Reinforced Concrete Columns. His research interests include biaxially loaded columns, column slenderness, and concrete-filled steel tube columns.

Cheng-Tzu Thomas Hsu, *FACI*, is a professor and Director of the Structures Laboratories in the Department of Civil and Environmental Engineering, New Jersey Institute of Technology, Newark, N.J. He is a member of ACI Committees 435, Deflection of Building Structures; 444, Experimental Analysis; and Joint ACI-ASCE Committee 441, Reinforced Concrete Columns.

S. Ali Mirza, *FACI*, is a professor of civil engineering at Lakehead University, Thunder Bay, Ontario, Canada. He is a member of ACI Committees 335, Composite and Hybrid Structures; 340, Design Aids for ACI Building Codes; 408, Bond and Development of Reinforcement; and Joint ACI-ASCE Committee 441, Reinforced Concrete Columns. He is a recipient of the ACI Structural Research Award.

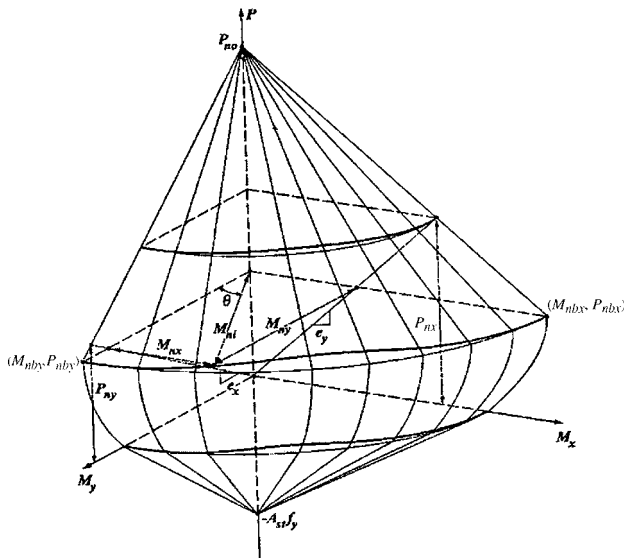


Fig. 1—Typical interaction surface for ultimate strength of column cross section.

Deviations from the elliptical approximation are largest when the ultimate axial load is near the axial load strength corresponding to a balanced strain condition and the eccentricity of the axial load is in the direction of a corner of the cross section. The balanced strain condition occurs when a limiting strain of 0.003 in the concrete is reached as the tension reinforcement achieves first yield. Design aids were developed from analyses that used the rectangular stress block for concrete.⁹⁻¹¹ The design aid relationship used was

$$\left[\frac{M_{nx}}{M_{x0}} \right]^\alpha + \left[\frac{M_{ny}}{M_{y0}} \right]^\alpha = 1 \quad (1a)$$

where

M_{nx} = applied nominal bending moment about the X-axis;
 M_{x0} = nominal bending moment strength if axial load were eccentric only about the X-axis;
 M_{ny} = applied nominal bending moment about the Y-axis;
 M_{y0} = nominal bending moment strength if axial load were eccentric only about the Y-axis; and
 α = axial load contour exponent between 1 and 2.

Equation (1a) describes the true ellipse when the exponent $\alpha = 2$, and can be written as

$$\left[\frac{M_{nx}}{M_{x0}} \right]^2 + \left[\frac{M_{ny}}{M_{y0}} \right]^2 = 1 \quad (\text{The Elliptic Load Contour Equation}) \quad (1b)$$

Graphs in Reference 10 show α to be a function of the ratio between the specified compressive strength of concrete and the yield strength of steel, the ratio between the ultimate axial load and the cross section ultimate concentric strength, the reinforcement ratio, and the ratio between the shorter and the longer side of a rectangular cross section.

Design aids in the 1970 ACI SP-17A Handbook¹² and the 1972 *CRSI Handbook*¹³ were based on interaction diagrams developed in Reference 14 for square cross sections bent about the diagonal axis at 45 degrees for which the resultant moment acts in a plane of symmetry. The contour for an axial load on the interaction surface was defined by two straight lines that connect moment values for bending about a principal axis and the moment value at the 45-degree skew angle.

An alternate equation that can be used to describe an ultimate strength interaction surface published in 1960¹⁵ and is used in the commentary of ACI 318⁶ as evidence of adequate strength in reinforced concrete cross sections

$$\frac{1}{P_{ni}} = \frac{1}{P_{nx}} + \frac{1}{P_{ny}} - \frac{1}{P_{n0}} \quad (\text{The Reciprocal Load Equation}) \quad (2)$$

where

P_{ni} = nominal axial load strength under biaxial eccentricity;
 P_{nx} = nominal axial load strength for single eccentricity along Y-axis;
 P_{ny} = nominal axial load strength for single eccentricity along X-axis; and
 P_{n0} = nominal concentric compression strength of the cross section.

If the value of P_{ni} from Eq. (2), reduced by a strength reduction factor ϕ , exceeds the applied factored axial load P_{ui} at the biaxial eccentricity, the section is adequate. Design aids in the 1978 ACI SP-17 Handbook¹⁶ were provided for solving Eq. (2). The use of Eq. (1) or (2) requires determining the cross section bending strength about each principal axis separately. Such definitions are available with design aids in the form of graphs¹⁷ or tables.¹⁸ Equation (1) and (2) were developed for cross section strength. These equations are also relevant for slender columns as for short columns if the values M_{nx} and M_{ny} for Eq. (1) and P_{nx} and P_{ny} for Eq. (2) are obtained with eccentricities magnified separately for bending and slenderness about each principal axis.

Reports of physical tests on square columns subjected to biaxially eccentric compression confirm the shape of interaction surfaces predicted from design aids and Eq. (1) and (2).¹⁹ Generally, test strengths exceeded strength predictions from the design aids. Studies on rectangular and round-ended bridge pier columns²⁰ included tests and analytical investigation, which used discrete elements and various stress-strain models for concrete. Ultimate strength estimates were found to be insensitive to the specific shape of the stress-strain function (bilinear, parabolic, higher-order polynomial) used for concrete in compression.²⁰ The clear spacing between longitudinal bars in these specimens was about 2 in. (51 mm) or less, and the effect such spacing can have on confining concrete effectively to develop more compression capacity was not considered.^{21,22} The test results showed that to predict the maximum bending moments between the ends of an eccentrically loaded slender column, moment magnifiers for slenderness effects could be evaluated separately for each principal axis of bending. Equation (1b) predicted ultimate biaxial strength of cross sections with an accuracy as precise

as that obtained with the rectangular concrete stress block applied for determining uniaxial strength.²⁰

The 1988 Australian Standard AS 3600²³ adopted Eq. (1a) for cross sectional strength with α being between 1 and 2 and defined as

$$\alpha = 0.7 + \frac{1.7P_{ui}}{0.6P_{n0}} \quad (\text{The Australian Standard}) \quad (3)$$

where

P_{ui} = applied factored axial load under biaxial eccentricity;

$\alpha = 1$ for values of P_{ui} less than $0.106P_{n0}$; and

$\alpha = 2$ for P_{ui} greater than $0.459P_{n0}$.

The 1983 AASHTO specifications²⁴ for highway structures accepted the results of cross sectional analysis derived from the same ultimate strength conditions as those in ACI 318,⁶ that is, a limit strain of concrete of 0.003, plane sections remaining plane during all load cases, equivalent rectangular compression stress block for concrete at ultimate strength, and elastic steel response before nominal yield strain with yield stress for all strains higher than or equal to nominal yield strain. In addition, when P_{ui} is greater than $0.1f'_c A_g$, Eq. (2) can be used; when P_{ui} is less than $0.1f'_c A_g$, Eq. (1a) with α equal to 1 can be used, where A_g = gross area of column cross section and f'_c = specified compressive strength of concrete.

Hsu²⁵ proposed a variation of Eq. (1) with the coefficient α equal to 1.5 and a term reflecting the influence of the ratio between the nominal axial load and balanced strain axial load

$$\left[\frac{P_{ni} - P_{nb}}{P_{n0} - P_{nb}} \right] + \left[\frac{M_{nx}}{M_{nbx}} \right]^{1.5} + \left[\frac{M_{ny}}{M_{nby}} \right]^{1.5} = 1.0 \quad (4)$$

(The Equation of Failure Surface)

where

P_{nb} = nominal axial load strength of the cross section for balanced strain condition under biaxial bending;

M_{nbx} = nominal bending moment strength for balanced strain condition if axial load were eccentric only about the X-axis; and

M_{nby} = nominal bending moment strength for balanced strain condition if axial load were eccentric only about the Y-axis.

The magnitude of P_{nb} will not be a constant value unless the column section is square and the same amount of longitudinal steel is placed on each of the four faces. The value of P_{nb} for Eq. (4) is between P_{nbx} for bending about the X-axis and P_{nby} for bending about the Y-axis. Linear interpolation is recommended.

Based on reports of the European Working Commission, MacGregor²⁶ suggested that sections designed for biaxial bending be proportioned on the basis of the required axial load acting at an eccentricity e_{oi} larger than either of the required values e_x and e_y . For e_x/x greater than or equal to e_y/y , a value e_{oi} should be taken as

$$e_{oi} = e_x + \beta e_y (x/y) \quad (5)$$

where with $P_u/(f'_c A_g) \leq 0.4$, $\beta = [0.5 + P_u/(f'_c A_g)](f_y + 40)/100 \geq 0.6$; with $P_u/(f'_c A_g) > 0.4$, $\beta = [1.3 - P_u/(f'_c A_g)](f_y + 40)/100 \geq 0.5$

(f_y in ksi units); A_g = gross area of cross section; and x, y = column cross section dimension along the X- and Y-axis, respectively.

If $e_x/x < e_y/y$, the x and y terms as well as the subscripts in Eq. (5) are transposed. Hence, a section is selected for the required load P_u acting at an eccentricity e_{oi} about one of the principal axes of the rectangular section. This procedure is limited in application to columns with doubly symmetric cross sections having the ratio of longer to shorter dimensions between 1 and 2 and reinforced with equal reinforcement on all four faces. As a result, it appears to be more suited for selection of trial sections for preliminary sizing of columns.

ULTIMATE STRENGTHS FROM DESIGN PROCEDURES COMPARED WITH TEST RESULTS

Ultimate axial load strengths from 59 test specimens subjected to biaxial bending from Bresler,¹⁵ Ramamurthy,¹⁹ Furlong,²⁰ Anderson and Lee,²⁷ Hsu,²⁵ and Heimdahl and Bianchini²⁸ were compared with those computed from the design formulas given previously. These formulas consist of Eq. (1b), Eq. (2), Eq. (1a) with α computed from Eq. (3), and Eq. (4). The refinements given in design aids of References 9 to 11 for determining the specific values of exponent α between 1 and 2 for Eq. (1a) produced computed strength values lower than those from Eq. (1b). The database involves column specimens with cross sections of 4 x 4 in. (101.6 x 101.6 mm) square to 8 x 8 in. (203.2 x 203.2 mm) square or 6 x 12 in. (152.4 x 304.8 mm) rectangle. Effective length varied from 16 to 80 in. (406.4 to 2032 mm). Reinforcement ratios ρ_g varied from 2.4 to 5% with yield strengths f_y from 44,500 to 73,000 psi (307 to 503 MPa). Concrete strength f'_c varied from 2805 to 5435 psi (19.3 to 37.5 MPa).

Computed strengths were determined using the concrete rectangular stress block of ACI 318 Section 10.2.7.⁶ Strength reduction factors ϕ were taken as 1.00 in computation. A computer program was prepared to evaluate strengths using singular applications of Eq. (1) to (4). Specimens were loaded symmetrically with respect to the midheight of the column and, for the purpose of data comparison, moment magnifiers were determined separately for each axis of bending. Hence, the factor δ_{ns} for each axis of bending was calculated from the approximation given in ACI 318 Section 10.12.3⁶ for columns in nonsway frames with P_u/ϕ taken as P_{ni} and the equivalent uniform moment diagram factor C_m taken as 1.0 for these specimens

$$\delta_{ns} = \frac{1}{1 - \frac{P_{ni}}{P_c}} \geq 1.0 \quad (6)$$

where $P_c = \pi^2 EI / (k\ell_u)^2$; k = the effective length factor taken as 1.0 for these tests; and EI = the larger value from $EI = (0.2E_c I_g + E_s I_s) / (1 + \beta_d)$ or $EI = 0.4E_c I_g / (1 + \beta_d)$ with $E_s = 33w_c^{1.5} \sqrt{f'_c}$ psi (w_c is the unit weight of concrete in lb/ft³, f'_c in psi) or $E_s = 0.043w_c^{1.5} \sqrt{f'_c}$ MPa (w_c is the unit weight of concrete in kg/m³, $\sqrt{f'_c}$ in MPa), $E_s = 29 \times 10^6$ psi (200,000 MPa), and $\beta_d = 0$ (short-term load). As indicated by Eq. (6), the stiffness reduction factor ϕ_k used in ACI 318⁶ Eq. (10-9) was taken equal to 1.0 for this study. Table 1 displays the specimen properties, observed strengths (measured axial load strengths P_{test}), and the ratios between the observed strengths and the computed axial load strengths (P_1, P_2, P_3, P_4). P_1 was computed using Eq. (1b), P_2 was calculated using Eq. (2), P_3 was evaluated from Eq. (1a) with α taken

from Eq. (3), and P_4 was determined from Eq. (4). Average values of ratios between observed strengths and computed strengths from each of the four design equations are given at the bottom of Table 1 together with the standard deviation and the coefficient of variation for each set of ratios. The average values of ratios between the observed and calculated strengths are 0.98 for P_1 , 1.07 for P_2 and P_4 , and 1.16 for P_3 .

The coefficients of variation are nearly 0.16 for P_1 , P_2 , and P_4 , and 0.2 for P_3 . These values show reasonable agreement between observed and calculated strengths, indicating that all four methods of calculation compared in Table 1 are acceptable for design. A similar conclusion was drawn by Amirthanandan and Rangan²⁹ for the Australian Standard AS3600.²³ Sample calculations for a test specimen taken

Table 1—Comparison of observed and computed axial load strengths

Reference	$b \times h$, mm x mm	kl_u , m	ρ_g , %	f_y , MPa	f'_c , MPa	e_x , mm	e_y , mm	P_{test} , kN	P_{test}/P_1	P_{test}/P_2	P_{test}/P_3	P_{test}/P_4
15	152 x 203	1.21	2.6	368.9	22.1	76.2	101.6	142.3	0.831	0.979	1.131	0.950
					25.5	152.4	203.2	75.6	0.971	1.278	1.441	1.000
					24.1	152.4	101.6	93.4	0.968	0.909	1.333	0.968
					24.8	76.2	203.2	106.8	0.992	1.472	1.437	1.076
19	203 x 203	2.03	3.9	322.6	29.2*	21.0	78.5	628.9	1.114	1.201	1.130	1.179
					25.8*	19.4	46.9	771.7	1.075	1.177	1.075	1.225
					33.5*	50.8	88.0	533.8	1.079	1.108	1.217	1.145
					32.0*	63.5	110.0	395.9	1.040	1.094	1.280	1.050
					19.5*	35.9	35.9	598.3	0.980	1.114	0.980	1.151
					27.6*	64.7	64.7	500.4	0.996	1.046	1.065	1.089
					29.5*	71.8	71.8	516.0	1.096	1.148	1.249	1.185
					34.1*	101.6	101.6	369.6	1.092	1.187	1.497	1.090
	152 x 229	1.91	4.6	322.6	31.6*	25.4	38.1	785.1	1.164	1.293	1.164	1.351
					25.4*	55.7	84.5	400.3	1.132	1.233	1.281	1.253
					24.5*	76.2	114.3	311.4	1.207	1.331	1.559	1.296
					25.1*	32.3	32.3	680.5	1.233	1.362	1.235	1.406
					30.9*	80.8	80.8	378.1	1.127	1.200	1.399	1.320
					23.9*	79.2	45.7	400.3	1.327	1.367	1.454	1.374
	152 x 305	1.91	3.4	322.6	23.4*	56.8	113.6	464.8	1.225	1.281	1.451	1.348
					21.4*	76.2	152.4	311.4	1.112	1.214	1.452	1.190
					27.7*	86.2	86.2	435.9	1.374	1.422	1.658	1.352
					24.8*	66.0	38.1	542.7	1.294	1.287	1.351	1.308
20	127 x 229	1.93	2.4	451.6	33.7	26.4	10.2	529.3	1.059	1.091	1.061	1.201
					33.6	19.1	22.9	533.8	0.952	1.014	0.952	1.096
					35.7	12.7	38.4	573.8	0.942	1.024	0.942	1.097
					34.5	28.7	9.9	387.4	0.799	0.822	0.800	0.898
					35.9	26.2	30.7	419.4	0.847	0.907	0.854	0.962
					32.4	18.5	56.4	381.6	0.817	0.899	0.825	0.932
					30.5	47.2	20.3	239.7	0.717	0.709	0.730	0.791
					30.0	54.9	49.0	179.7	0.635	0.653	0.693	0.697
					30.7	41.4	110.5	179.7	0.707	0.770	0.874	0.757
27	102 x 102	1.27	5	314.4	37.5	71.6	71.6	60.0	0.839	0.925	1.189	0.818
					37.5	71.6	71.6	64.5	0.901	0.993	1.278	0.879
25	102 x 102	0.76	2.75	306.8	22.1	25.4	38.1	93.4	0.886	1.034	0.938	0.968
					28.2	25.4	38.1	110.3	0.908	0.963	0.961	1.002
		1.02	2.81	503.3	26.9	63.5	88.9	42.7	1.000	1.171	1.433	1.061
					26.2	76.2	88.9	38.7	0.981	1.18	1.426	1.048
					26.8	88.9	88.9	35.6	0.964	1.176	1.408	1.027
					26.4	50.8	50.8	63.6	0.947	1.039	1.312	1.057
					25.6	12.7	101.6	48.0	1.059	1.049	1.191	1.049
					26.9	12.7	17.8	27.8	1.102	1.099	1.186	1.026
	108 x 108	1.62	4.87	306.8	24.4	76.2	50.8	61.8	1.073	1.214	1.487	1.094
					26.8	82.6	57.2	52.5	0.971	1.113	1.353	0.971
					29.1	63.5	76.2	60.5	1.075	1.248	1.520	1.075

*Based on $f'_c = 0.9f_{cu}$, where f_{cu} is compressive strength of 150 mm cubes.

Note: Smaller dimension of cross section is along X-axis and larger dimension of cross section is along Y-axis; e_x is eccentricity along X-axis and e_y is eccentricity along Y-axis (both acting at column ends); and k is effective length factor that is equal to 1.0.

Table 1 (cont.)—Comparison of observed and computed axial load strengths

Reference	$b \times h$, mm x mm	$k\ell_u$, m	ρ_g , %	f_y , MPa	f'_c , MPa	e_x , mm	e_y , mm	P_{test} , kN	P_{test}/P_1	P_{test}/P_2	P_{test}/P_3	P_{test}/P_4
28	127 x 127	0.41	3.2	493.7	31.9	10.4	25.1	324.7	0.825	0.903	0.825	1.150
					31.9	10.4	25.0	342.5	0.869	0.952	0.869	1.110
					31.9	19.4	19.4	347.8	0.884	1.000	0.884	1.205
					31.9	19.2	19.2	335.8	0.927	1.046	0.927	1.196
		0.76	3.2	493.7	34.5	66.6	27.6	169.0	0.875	0.990	0.944	0.997
					34.5	124.2	51.4	85.0	0.816	0.827	1.091	0.864
					34.5	127.7	52.9	78.3	0.779	0.793	1.038	0.842
					35.6	48.2	48.2	172.1	0.823	0.975	0.956	0.958
					35.6	49.5	49.5	164.6	0.806	0.956	0.948	0.944
					35.6	96.1	96.1	82.3	0.796	0.883	1.169	0.855
					35.6	94.6	94.6	84.1	0.797	0.879	1.216	0.883
					24.0	63.6	26.3	187.3	1.096	1.253	1.153	1.349
					24.0	124.2	51.4	82.3	0.877	1.034	1.101	0.934
					25.2	48.7	48.7	169.9	0.995	1.197	1.127	1.205
					25.2	94.3	94.3	81.0	0.854	1.017	1.152	0.943
					Average				0.977	1.076	1.164	1.072
					Standard deviation				0.158	0.178	0.234	0.169
					Coefficient of variation				0.162	0.166	0.201	0.158

Note: Smaller dimension of cross section is along X-axis and larger dimension of cross section is along Y-axis; e_x is eccentricity along X-axis and e_y is eccentricity along Y-axis (both acting at column ends); and k is effective length factor that is equal to 1.0.

from Furlong²⁰ and listed in Table 1 are shown in Appendix A.

COMPUTER-BASED ANALYSIS PROCEDURES

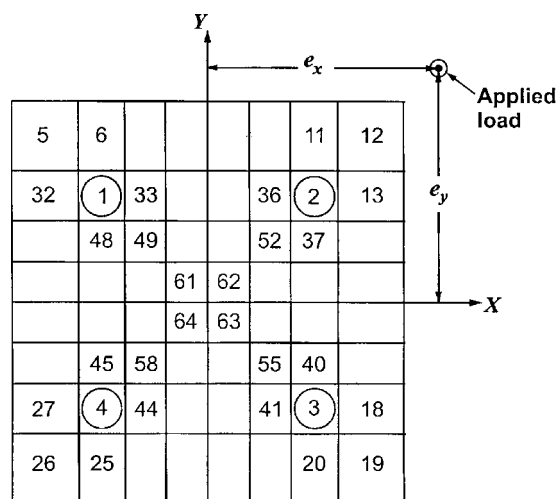
Anticipating the availability of computers for design and recognizing that, for an assumed level of axial load and skew angle of a neutral axis, an iterative procedure is programmable for determining appropriate moment values M_{nx} and M_{ny} . Taylor³⁰ proposed that several values of M_{nx} and M_{ny} should be computed to define a moment strength contour for the given axial load. Linear interpolation between computed points would give the strength value for the desired skew angle. Taylor's method represents a transition between approximate design by formulas and analysis for design with help from computer programs.

Ultimate strength

Several numerical procedures³¹⁻³³ suited for computer use were developed to perform an analysis based on force equilibrium and strain compatibility for columns with cross sections of arbitrary shape. A common procedure produces a set of points for a constant ratio of bending moments M_x and M_y (constant skew angle) on the three-dimensional failure surface for constructing the resulting interaction lines (Fig. 1). The use of computers permits an iterative process that is as time efficient as the approximate design procedures described previously and elsewhere.^{26,34-39}

Moment-curvature and load-deflection behavior

Computer analyses of column cross sections are based on force equilibrium, strain compatibility, and stress-strain relationships for the constituent materials. Special conditions, such as concrete confinement and/or strain-hardening of steel, can be included. Most methods involve the subdivision of the cross section into elements as shown in Fig. 2. Each element is assumed to have either a constant stress or a linearly varying stress. It is necessary to assume the location and orientation of the axis of zero strain. Strains are propor-



Elements 1 to 4 represent longitudinal reinforcing steel.
Elements 5 to 32 represent unconfined concrete.
Elements 33 to 64 represent confined concrete.

Fig. 2—Discretized cross section of square column for computer analysis.

tional to the distance from the zero strain axis. Stresses are obtained from stress-strain relationships for the concrete and steel. With the force in each element known, the resultant axial force and bending moments about the two axes can be calculated. Several iterations of the neutral axis position are generally needed before the axial force and bending moments conform to the desired convergence. Any of the several computational techniques available,⁴⁰⁻⁴⁸ such as tangent and second stiffness methods, can be used to produce acceptable strength results.

Most methods of computer analysis include the following assumptions for the cross section (Fig. 2) and for the member (Fig. 3): 1) plane sections remain plane during bending; 2) stress-strain relationships for the constituent materials are known; 3) effects of axial and shear deformations are negligible;

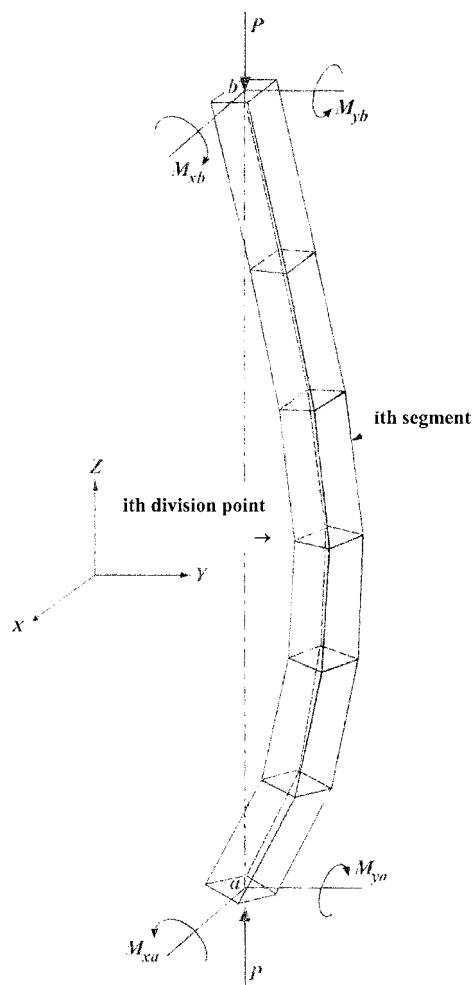


Fig. 3—Slender column divided into segments.

4) no slip takes place between the steel and the surrounding concrete; 5) end-restraint conditions for the member are known; 6) under zero loading, the segment lengths are straight; and 7) under eccentric load, the curvature is constant for each segment.

For a displacement-controlled computer analysis of slender columns subjected to symmetric single curvature (Fig. 3), a value of deflection at any point, usually the midheight, along the minor axis is assigned, and a trial set of axial load and end bending moments is assumed. Then, the internal moments, including the second-order moments due to lateral deflection of the member are calculated at each division point. The curvature and the distribution of strains at each division point can be obtained from the moment-curvature diagram developed for the cross section. Material nonlinearity is included through the stress-strain curves. Cracking of concrete is also included through the tensile stress-strain curve of concrete. The second stiffness method is employed to capture the nonlinear material behavior. Curvatures along the column length are either integrated numerically to obtain deflection at all division points, or a finite difference approach is used to formulate the relationship between the curvature and the deflection. If the calculated deflection at midheight does not agree with the assumed value, the trial set of axial load and end bending moments is modified, and the procedure is repeated until the convergence is within an acceptable limit, normally 0.1% of the assumed deflection.

For the first iteration, the deflection for each division point is initially assumed to be zero, or assigned any other value

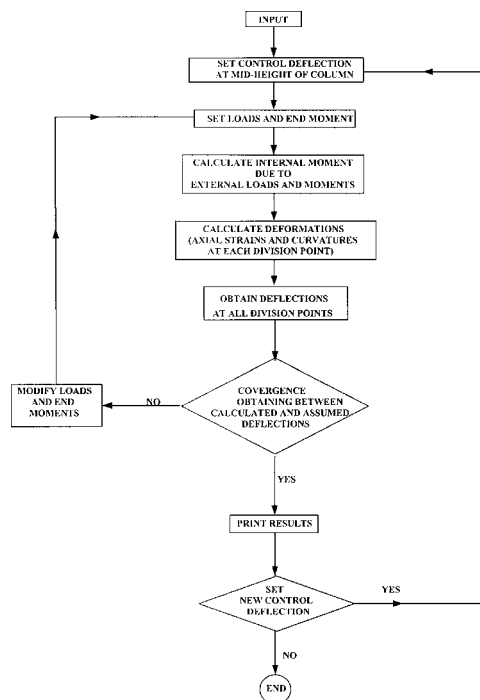


Fig. 4—Flow chart for analysis of slender columns.

close to zero, and the resulting bending moments and deflections at all the division points are calculated. The calculated deflected shape is then taken as the assumed deflected shape for the subsequent iteration. After a solution is obtained corresponding to a particular value of assigned deflection at midheight, a new value of the midheight deflection is assigned and the whole procedure is repeated. This method, summarized in the flow chart of Fig. 4, is capable of determining both ascending and descending branches of the moment-curvature and load-deflection curves and has been successfully used for columns reported by Wang and Hsu,⁴⁶ Hsu and Mirza,⁴² Chen and Shoraka,⁴³ Al-Noury and Chen,⁴⁵ Poston, Breen, and Roeset;⁴⁷ and Menegotto and Pinto⁴⁸ also developed computer analysis methods using a tangent stiffness technique to evaluate the load-moment-deflection relationships. Their methods, however, can calculate the curvatures and deflections up to the maximum axial load capacity only. In other words, at present a tangent stiffness technique is not capable of handling the descending branch beyond the maximum load capacity.

Computed load-deflection and moment-curvature curves for two slender columns based on the procedures described previously are reported herein. Details of these columns—Column C4 taken from Reference 49 and Column RC7 taken from Reference 22—are given in Fig. 5. Figure 6 to 8 represent a comparison of analytical and experimental results that show good agreement between experiment and analysis. It is noted that the second stiffness method has been used to compare the behavior of tested Column C4 (Fig. 6 and 7), whereas the tangent stiffness method is employed to compare the behavior of tested Column RC7 (Fig. 8).

ULTIMATE STRENGTHS FROM COMPUTER-BASED ANALYSIS COMPARED WITH TEST VALUES

Ultimate axial-load strengths from 20 column specimens tested under biaxial bending from Bresler,¹⁵ Ramamurthy,¹⁹ Anderson and Lee,²⁷ and Hsu²⁵ were compared with the computer-based analysis procedure. The procedure and

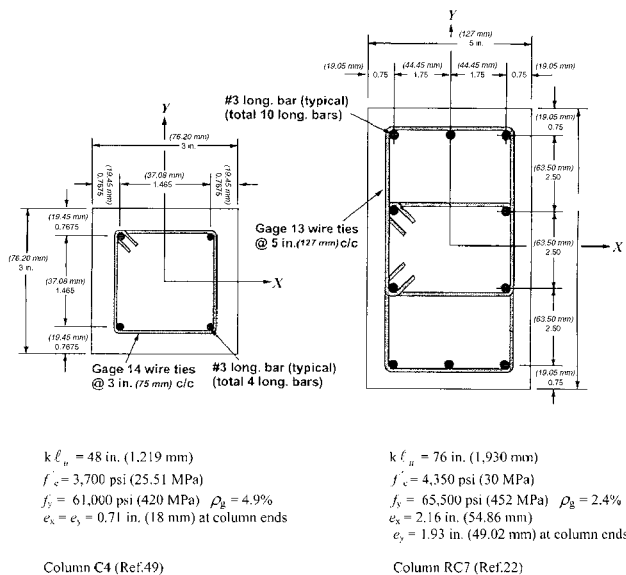


Fig. 5—Details of Columns C4 and RC7 (diameter of No. 3 bar = 9.5 mm; diameter of Gage 14 wire = 0.08 in. (2.03 mm); diameter of Gage 13 wire = 0.0915 in. (2.32 mm); 10 in. = 254 mm; 1000 psi = 6.9 MPa).

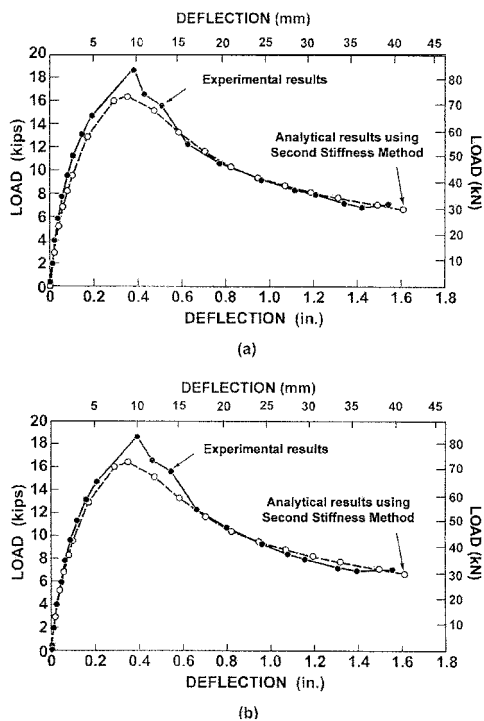


Fig. 6—Comparison of load-deflection curves for Column C4 at midheight using second stiffness method for: (a) deflection in X-direction; and (b) deflection in Y-direction (Reference 49).

underlying assumptions used for the computer analysis are described previously.

Table 2 lists specimen details, observed ultimate axial-load strengths P_{test} , ultimate axial-load strengths from the computer-based analysis P_{comp} , and values of the ratio P_{test}/P_{comp} . For the purpose of comparison with P_{test}/P_{comp} , Table 2 also shows values of P_{test}/P_1 , P_{test}/P_2 , P_{test}/P_3 , and P_{test}/P_4 , which were taken from Table 1 and calculated from design equations described previously. In addition, Table 2 shows the statistics for P_{test}/P_{comp} , P_{test}/P_1 , P_{test}/P_2 , P_{test}/P_3 , and

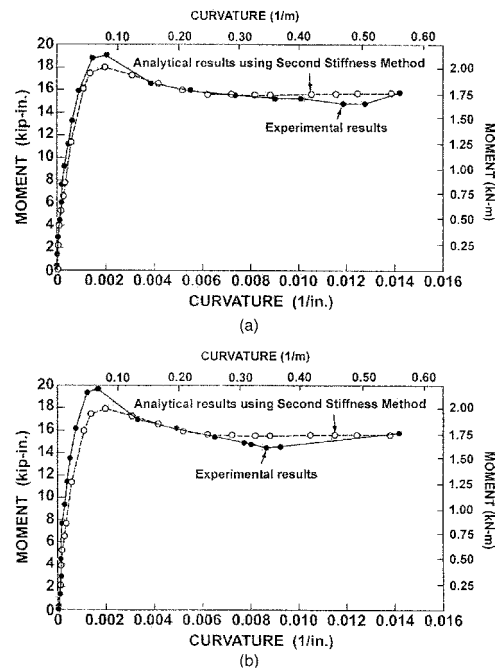


Fig. 7—Comparison of moment-curvature curves for Column C4 at midheight using second stiffness method for: (a) bending moment about X-axis; and (b) bending moment about Y-axis (Reference 49).

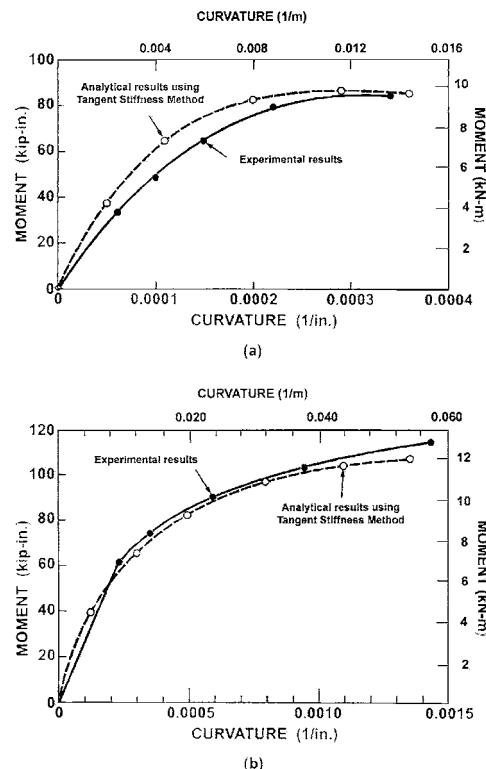


Fig. 8—Comparison of moment-curvature curves for Column RC7 at midheight using tangent stiffness method for: (a) bending moment about X-axis (strong axis); and (b) bending moment about Y-axis (weak axis) of column.

P_{test}/P_4 . A comparison of the average value and the coefficient of variation for P_{test}/P_{comp} with those for P_{test}/P_1 , P_{test}/P_2 , P_{test}/P_3 , and P_{test}/P_4 indicates the acceptability of the computer-analysis procedure.

Table 2—Comparison of observed axial-load strengths and axial load strengths computed from computer-based analysis procedure

Reference	$b \times h$, mm x mm	$k\ell_u$, m	ρ_g , %	f_y , MPa	f'_c , MPa	e_x , mm	e_y , mm	P_{test} , kN	P_{comp}^* , kN	P_{test}/P_{comp}	P_{test}/P_1	P_{test}/P_2	P_{test}/P_3	P_{test}/P_4
15	152 x 203	1.22	2.60	368.9	22.1	76.2	101.6	142.3	120.5	1.181	0.831	0.979	1.131	0.950
					25.5	152.4	203.2	75.6	62.9	1.202	0.971	1.278	1.441	1.000
					24.1	152.4	101.6	93.4	75.5	1.237	0.968	0.909	1.333	0.968
					24.8	76.2	203.2	106.8	88.3	1.209	0.992	1.472	1.437	1.076
19	203 x 203	2.03	3.90	322.6	25.8 [†]	19.4	46.9	771.7	770.9	1.019	1.075	1.177	1.075	1.225
					19.5 [†]	35.9	35.9	598.3	615.0	0.973	0.980	1.114	0.980	1.151
					34.1 [†]	101.6	101.6	369.6	367.2	1.007	1.092	1.187	1.497	1.090
27	101 x 102	1.27	5.00	314.4	37.5	71.6	71.6	60.0	63.0	0.953	0.839	0.925	1.189	0.818
					37.5	71.6	71.6	64.5	63.0	1.023	0.901	0.993	1.278	0.879
25	102 x 102	0.76	2.75	306.8	22.1	25.4	38.1	93.4	96.1	0.972	0.886	1.034	0.938	0.968
					28.2	25.4	38.1	110.3	110.4	0.999	0.908	0.963	0.961	1.002
		1.02	2.81	503.3	26.9	63.5	88.9	42.7	44.0	0.971	1.000	1.171	1.433	1.061
					26.2	76.2	88.9	38.7	40.3	0.959	0.981	1.180	1.426	1.048
					26.8	88.9	88.9	35.6	37.7	0.943	0.964	1.176	1.408	1.027
					26.4	50.8	50.8	63.6	66.5	0.957	0.947	1.039	1.312	1.057
					25.6	12.7	101.6	48.0	46.5	1.033	1.059	1.049	1.191	1.049
	26.9	12.7	177.8	27.8	27.5	1.10	1.102	1.099	1.186	1.026				
	108 x 108	1.62	4.87	306.8	24.4	76.2	50.8	61.8	60.2	1.027	1.073	1.214	1.487	1.094
					26.8	82.6	57.2	52.5	57.1	0.919	0.971	1.113	1.353	0.971
					29.1	63.5	76.2	60.5	59.9	1.010	1.075	1.248	1.520	1.075
Average										1.030	0.981	1.116	1.279	1.027
Standard deviation										0.096	0.081	0.136	0.187	0.090
Coefficient of variation										0.093	0.083	0.122	0.146	0.088

*Values of P_{comp} were taken from Reference 25.

[†]Based on $f'_c = 0.9f_{cu}$, where f_{cu} is compressive strength of 150 mm cubes.

Note: Smaller dimension of cross section is along X-axis and larger dimension of cross section is along Y-axis; e_x is eccentricity along X-axis and e_y is eccentricity along Y-axis (both acting at column ends); and k is effective length factor that is equal to 1.0.

COLUMNS OF NONRECTANGULAR CROSS SECTION

Irregularly shaped columns can result from architectural consideration or geometric limitations. Frequently, such columns are located at the exterior of structural systems and are subjected to a combination of axial-load and biaxial bending.

In the case of column and shearwall configurations, wide-flange sections have been used to enhance both strength and stiffness. L-sections are frequently located at the corners of buildings, channel sections are used as columns or enclosures of elevator shafts, and S- and X-sections have architectural functions. Current building codes provide specific assumptions for the analysis of both sections and members, but design aids are few in number because of the multiplicity of section geometries. Marin⁵⁰ and Park and Paulay³⁵ have developed design aids for L-sections and channel sections, respectively. Ramamurthy and Khan,⁵¹ Hsu,⁵²⁻⁵⁴ Poston et al.,⁵⁵ and Tsao and Hsu⁴⁹ have carried out tests on columns with various sections and complemented these tests with analyses and design equations. They show that the computer analyses of both tangent and second stiffness methods described previously are capable of predicting the load-deformation behavior of columns with nonrectangular cross section.

CONCLUDING REMARKS

Various methods of analyses have been reviewed and compared with test data obtained from tests on short and slender columns with various rectangular and square cross sections. It is concluded that the elliptic load contour equation,

Eq. (1b), and the reciprocal load equation, Eq. (2), are the simplest to use, as these formulations do not require supplementary calculations that reflect the influence of axial loads near the value of balanced axial load strength. The equation of failure surface, Eq. (4), includes such influence, but it produces average strength ratio, standard deviation, and coefficient of variation only marginally better than such values from the reciprocal load equation. The standard deviation and the coefficient of variation near 16% for the elliptic load contour equation suggests that in too many cases it will not be conservative. The same values near 17% for the reciprocal load equation and the equation of failure surface should be sufficiently conservative because the average of strength values are more than 7% higher than measured values. It is recommended that the reciprocal load equation and the equation of failure surface be used for verifying section strength. These equations are not helpful for selecting a column section. It should be noted that the equation of failure surface, Eq. (4), is able to attain the ultimate strengths not only for the concrete columns under biaxial loading, but also for the concrete columns under uniaxial bending. In addition, Eq. (4) can also be used to study the behavior of concrete columns subjected to combined biaxial bending and axial tension as well.

The elliptic load contour equation can be used effectively for help in selecting a column section. Because the ellipse equation appears to produce strength estimates less than those from the reciprocal load equation and the equation of failure surface, it is recommended that the resultant moment be

increased by 10% before the trial section is proportioned. If the column section is to be rectangular, the moment about the weak axis should be normalized by increasing its value by the ratio between long and short sides of the section before the resultant moment is computed for proportioning the section. A sample of examples can be found in Appendix B.

It is noted that the accuracy of the aforementioned design procedures for strength of slender columns depends on how the slenderness effect and the effect of sustained loads are accounted for in the computation of the member displacements. The second-order effect for the design of biaxially loaded slender columns can be improved by further observations from physical tests.

Various computer analyses that are able to determine both ultimate load and load-deformation behavior of concrete columns under biaxial bending are discussed herein. For practical purposes, a load-controlled computing technique along with the tangent stiffness method can be used to analyze the concrete columns up to maximum axial load capacity with any type of cross section. It spends less computing time than that of a displacement-controlled computing technique together with the second stiffness method. The second approach, however, is capable of capturing both ascending and descending branches of the load-deformation characteristics. It can be used for the detailed analysis and research on concrete column behavior under any combination of loadings.

ACKNOWLEDGMENTS

Acknowledgments are given to the following members of Joint ACI-ASCE Committee 441, Reinforced Concrete Columns, for their helpful suggestions: R. Green, D. D. Lee, J. G. MacGregor, and S. A. Sheikh.

REFERENCES

1. Large, G. E., *Reinforced Concrete Fundamentals*, Ronald Press, 1946, 334 pp.
2. Au, T., "Ultimate Strength Design of Rectangular Concrete Members Subject to Unsymmetrical Bending," *ACI JOURNAL, Proceedings* V. 54, No. 2, Feb. 1958, pp. 657-674.
3. Chu, K.-H., and Pabarcus, A., "Biaxially Loaded Reinforced Concrete Columns," *Journal of the Structural Division*, ASCE, V. 84, No. ST8, Dec. 1958, pp. 1-27.
4. Czerniak, E., "Analytical Approach to Biaxial Eccentricity," *Journal of the Structural Division*, ASCE, V. 88, No. ST4, Aug. 1962, pp. 105-158.
5. Whitney, C. S., "Plastic Theory of Reinforced Concrete Design," *ASCE Transactions* 107, 1942, p. 251.
6. ACI Committee 318, "Building Code Requirements for Structural Concrete (ACI 318-02) and Commentary (318R-02)," American Concrete Institute, Farmington Hills, Mich., 2002, 443 pp.
7. Pannell, F. N., "The Design of Biaxially Loaded Columns by Ultimate Load Methods," *Magazine of Concrete Research*, London, V. 12, No. 35, July 1960, pp. 103-104.
8. Furlong, R. W., "Ultimate Strength of Square Columns Under Biaxially Eccentric Loads," *ACI JOURNAL, Proceedings* V. 57, Mar. 1961, pp. 1129-1140.
9. Fleming, J. F., and Werner, S. D., "Design of Columns Subjected to Biaxial Bending," *ACI JOURNAL, Proceedings* V. 62, No. 3, Mar. 1965, pp. 327-342.
10. Parme, A.; Nieves, J. M.; and Gouwens, A., "Capacity of Reinforced Rectangular Columns Subject to Biaxial Bending," *ACI JOURNAL, Proceedings* V. 63, No. 9, Sept. 1966, pp. 911-923.
11. Aas-Jakobsen, A., "Biaxial Eccentricities in Ultimate Load Design," *ACI JOURNAL, Proceedings* V. 61, No. 3, Mar. 1964, pp. 293-316.
12. ACI Committee 340, *ACI Design Handbook: Columns*, V. 2, SP-17A, American Concrete Institute, Farmington Hills, Mich., 1970, 226 pp.
13. Concrete Reinforcing Steel Institute, *CRSI Handbook*, Chicago, 1972, pp. 2-1 to 4-74.
14. Weber, D. C., "Ultimate Strength Design Charts for Columns with Biaxial Bending," *ACI JOURNAL, Proceedings* V. 63, No. 11, Nov. 1966, pp. 1205-1230.
15. Bresler, B., "Design Criteria for Reinforced Columns under Axial Load and Biaxial Bending," *ACI JOURNAL, Proceedings* V. 57, No. 11, Nov. 1960, pp. 481-490.
16. ACI Committee 340, *ACI Design Handbook: Columns*, V. 2, SP-17A, American Concrete Institute, Farmington Hills, Mich., 1978, 214 pp.
17. Everard, N. J., and Cohen, E., *Ultimate Strength Design of Concrete Columns*, SP-7, American Concrete Institute, Farmington Hills, Mich., 1964, 182 pp.
18. CRSI Engineering Practice Committee, *Columns by Ultimate Strength Design*, Concrete Reinforcing Steel Institute, Chicago, 1967.
19. Ramamurthy, L. N., "Investigation of the Ultimate Strength of Square and Rectangular Columns Under Biaxially Eccentric Loads," *Reinforced Concrete Columns*, SP-13, American Concrete Institute, Farmington Hills, Mich., 1966, pp. 263-298.
20. Furlong, R. W., "Concrete Columns under Biaxially Eccentric Thrust," *ACI JOURNAL, Proceedings* V. 76, No. 10, Oct. 1979, pp. 1093-1118.
21. Mavichak, Viroj, "Strength and Stiffness of Reinforced Concrete Columns Under Biaxial Bending," PhD dissertation, the University of Texas at Austin, Austin, Tex., May 1977, 209 pp.
22. Mavichak, V., and Furlong, R. W., "Strength and Stiffness of Reinforced Concrete Columns under Biaxial Bending," *Research Report 7-2F*, Center for Highway Research, the University of Texas at Austin, Austin, Tex., 1976, 219 pp.
23. Standards Association of Australia, "Concrete Structures AS 3600-1988," North Sydney, N.S.W., Australia, 1988, 105 pp.
24. AASHTO, "Standard Specifications for Highway Bridges," 13th Edition, Washington, D.C., 1983.
25. Hsu, C. T. T., "Analysis and Design of Square and Rectangular Columns by Equation of Failure Surface," *ACI Structural Journal*, V. 85, No. 2, Mar.-Apr. 1988, pp. 167-179.
26. MacGregor, J. G., *Reinforced Concrete: Mechanics and Design*, 3rd Edition, Prentice-Hall, Upper Saddle River, N.J., 1997, 939 pp.
27. Anderson, P., and Lee, B. N., "A Modified Plastic Theory of Reinforced Concrete," *Bulletin* 33, V. 54, No. 19, University of Minnesota, Minneapolis, Minn., Apr. 1951, 44 pp.
28. Heimdahl, P. D., and Bianchini, A. C., "Ultimate Strength of Biaxially Eccentrically Loaded Concrete Columns Reinforced with High Strength Steel," *Reinforced Concrete Columns*, SP-50, American Concrete Institute, Farmington Hills, Mich., 1975, pp. 93-117.
29. Amirthanandar, K., and Rangan, B. V., "Strength of Reinforced Concrete Columns in Biaxial Bending," *Civil Engineering Transactions*, V. CE33, No. 2, Apr. 1991, pp. 105-110.
30. Taylor, M. A., "Direct Biaxial Design of Columns," *Journal of Structural Engineering*, ASCE, V. 111, No. 1, Jan. 1985, pp. 158-173.
31. Smith, J. C., "Biaxially Loaded Concrete Interaction Curve," *Computers and Structures*, No. 3, 1973, pp. 1461-1464.
32. Davister, M. D., "A Computer Program for Exact Analysis," *Concrete International*, V. 8, No. 7, July 1986, pp. 56-63.
33. Wang, C. K., "Solving the Biaxial Bending Problem in Reinforced Concrete by a Three-Level Iteration Procedure," *Microcomputers in Civil Engineering*, No. 3, 1988, pp. 311-320.
34. Ferguson, P. M.; Breen, J. E.; and Jirsa, J. O., *Reinforced Concrete Fundamentals*, 5th Edition, John Wiley & Sons, New York, 1988, 746 pp.
35. Park, R., and Paulay, T., *Reinforced Concrete Structures*, Wiley-Interscience, New York, 1975, 769 pp.
36. Wang, C. K., and Salmon, C. G., *Reinforced Concrete Design*, 6th Edition, Harper Collins, New York, 1998, 1028 pp.
37. Nilson, A. H., *Design of Concrete Structures*, 12th Edition, McGraw-Hill, New York, 1997, 780 pp.
38. Leet, K., and Bernal, D., *Reinforced Concrete Design*, 3rd Edition, McGraw-Hill, New York, 1997, 546 pp.
39. Nawy, E. G., *Reinforced Concrete: A Fundamental Approach*, 3rd Edition, Prentice-Hall, Englewood Cliffs, N.J., 1996, 832 pp.
40. Cranston, W. B., "Determining the Relation Between Moment, Axial Load, and Curvature for Structural Members," *Technical Report TRA 395*, Cement and Concrete Association, London, June 1966, 11 pp.
41. Farah, A., and Huggins, M., "Analysis of Reinforced Concrete Columns Subjected to Longitudinal Load and Biaxial Bending," *ACI JOURNAL, Proceedings* V. 66, No. 7, July 1969, pp. 569-603.
42. Hsu, C. T., and Mirza, M. S., "Structural Concrete—Biaxial Bending and Compression," *Journal of the Structural Division*, ASCE, V. 99, No. ST2, Feb. 1973, pp. 285-290.
43. Chen, W. F., and Shoraka, M. T., *Tangent Stiffness Method for Biaxial Bending of Reinforced Concrete Columns*, IABSE Publications, V. 35-1, 1975, pp. 23-44.
44. Rotter, J. M., "Rapid Exact Inelastic Biaxial Bending Analysis," *Journal of Structural Engineering*, ASCE, V. 111, No. 12, Dec. 1985, pp. 2659-2674.
45. Al-Noury, S. I., and Chen, W. F., "Finite Segment Method for Biaxially Loaded RC Columns," *Journal of Structural Engineering*, ASCE, V. 108, No. 4, Apr. 1982, pp. 780-799.

46. Wang, G. G., and Hsu, C. T. T., "Complete Biaxial Load-Deformation Behavior of RC Columns," *Journal of Structural Engineering*, ASCE, V. 118, No. 9, Sept. 1992, pp. 2590-2609.
47. Poston, R. W.; Breen, J. E.; and Roeset, J. M., "Analysis of Nonprismatic or Hollow Slender Concrete Bridge Piers," *ACI JOURNAL, Proceedings* V. 82, No. 5, Sept.-Oct. 1985, pp. 731-739.
48. Menegotto, M., and Pinto P. E., "Slender RC Compressed Members in Biaxial Bending," *Journal of the Structural Division*, ASCE, V. 103, No. ST3, Mar. 1977, pp. 587-605.
49. Tsao, W. H., and Hsu, C. T. T., "Behavior of Biaxially Loaded Square and L-Shaped Slender Reinforced Concrete Columns," *Magazine of Concrete Research*, V. 46, No. 169, Dec. 1994, pp.257-267.
50. Marin, J., "Design Aids for L-Shaped Reinforced Concrete Columns," *ACI JOURNAL, Proceedings* V. 76, No. 11, Nov. 1979, pp. 1197-1216.
51. Ramamurthy, L. N., and Khan, T. A. H., "L-Shaped Column Design under Biaxial Eccentricity," *Journal of Structural Engineering*, ASCE, V. 109, No. 8, Aug. 1983, pp. 1903-1917.
52. Hsu, C. T. T., "Biaxially Loaded L-Shaped Reinforced Concrete Columns," *Journal of Structural Engineering*, ASCE, V. 111, No. 12, Dec. 1985, pp. 2576-2595; Errata, V. 114, No. 11, Nov. 1988, p. 2629.
53. Hsu, C. T. T., "Channel-Shaped Reinforced Concrete Compression Members under Biaxial Bending," *ACI Structural Journal*, V. 84, No. 3, May-June 1987, pp. 201-211; Errata, V. 85, No. 3, May-June 1988, p. 240.
54. Hsu, C. T. T., "T-Shaped Reinforced Concrete Members under Biaxial Bending and Axial Compression," *ACI Structural Journal*, V. 86, No. 4, July-Aug. 1989, pp. 460-468.
55. Poston, R. W.; Gilliam, T. E.; Yamamoto, Y.; and Breen, J. E., "Hollow Concrete Bridge Pier Behavior," *ACI JOURNAL, Proceedings* V. 82, No. 6, Nov. 1985, pp. 779-787.

APPENDIX A

Example calculations for strength estimates

Sample calculations for the 5th test specimen listed in Table 1 from Furlong²⁰ are shown as follows. For the Furlong test specimens, 76 in.-long (1930 mm) columns with a section 5 in. (127 mm) wide and 9 in. (229 mm) thick, were reinforced with 10 No. 3 longitudinal bars that had a yield strength $f_y = 65,500$ psi (448 MPa). The 5th test specimen had a concrete strength $f'_c = 5210$ psi (36.0 MPa), and the axial force was located 1.03 in. (26.2 mm) from the minor axis and 1.21 in. (30.7 mm) from the major axis. The centers of No. 3 longitudinal bars were reported to be located 0.75 in. (19.1 mm) from the edge of the section. For all methods, the values EI_x and EI_y must be computed to determine values P_{cx} and P_{cy} for moment magnification.

For this specimen, use $E_c = 57,600 \sqrt{f'_c} = 57,600 \sqrt{5210} = 4,160,000$ psi (28.7 GPa); $EI_x = (4160/5)[5(9)^3/12] + (29,000)[6(0.11)(4.5 - 0.75)^2 + 4(0.11)(1.25)^2] = 542,000$ kip-in.² (1555.5 kN-m²); and $EI_y = (4160/5)[9(5)^3/12] + (29,000)8(0.11)(2.5 - 0.75)^2 = 156,000$ k-in.² (447.7 kN-m²).

The value P_{cx} for buckling about the major axis: $P_{cx} = \pi^2 EI_x / \ell^2 = 926$ kips (4118.8 kN).

The value P_{cy} for buckling about the minor axis: $P_{cy} = \pi^2 EI_y / \ell^2 = 267$ kips (1187.6 kN).

Moment magnification factors will apply with minor axis bending in symmetric single curvature. For all methods,

strength interaction data for this specimen were developed. These data are shown in Table A-1.

Method 1—Eq. (1b): The elliptic load contour equation

This method requires iteration to determine the axial force for which moments will satisfy Eq. (1).

Trial 1, for $P_n = 94.3$ kips (419.4 kN), the reported test load capacity, end eccentricity along major axis = 1.03 in. (26.2 mm), and end eccentricity along minor axis = 1.21 in. (37.2 mm).

Applying moment magnifier $\delta_{ns} = 1/(1 - P/P_c)$, $\delta_{nsx} M_{nx} = [1/(1 - 94.3/926)]94.3(1.21) = 127.0$ kip-in. (14.35 kN-m), and $\delta_{nsy} M_{ny} = [1/(1 - 94.3/267)]94.3(1.03) = 150.2$ kip-in. (16.97 kN-m).

Table A1 gives for $P_n = 94.3$ kips (419.4 kN), $M_{x0} = 94.3(3.99) = 376.3$ kip-in. (42.5 kN-m), and $M_{y0} = 94.3(2.35) = 221.6$ kip-in. (25.0 kN-m). Equation (1b) becomes $(127.0/376.3)^2 + (150.2/221.6)^2 = 0.573$, indicating that the failure load is larger than 94.3 kips (419.4 kN). Iteration shows that when $P_n = 111.3$ kips (495.1 kN), Eq. (1) = 1. For $P_n = 111.3$ kips (495.1 kN), $M_{nx} = [1/(1 - 111.3/926)]111.3(1.21) = 153.1$ kip-in. (17.3 kN-m) and $M_{ny} = [1/(1 - 111.3/267)]111.3(1.03) = 196.6$ kip-in. (22.2 kN-m).

Table A1 for $P_n = 111.3$ kips (495.1 kN) gives $M_{x0} = 111.3(3.31) = 368$ kip-in. (41.6 kN-m) and $M_{y0} = 111.3(1.95) = 217$ kip-in. (24.5 kN-m). Equation (1b) then gives $(153.1/368)^2 + (196.6/217)^2 = 0.994$, indicating that the failure load is 111.3 kips (495.1 kN).

Method 2—Eq. (2): The reciprocal load equation

This equation would be quite convenient if slenderness effects were not to be considered. Because critical eccentricities at midheight must include slenderness effects, however, use the test load as a trial value for P_{ni} . Moment magnification factors determined for Method 1 for the axial force of 94.3 kips (419.4 kN) can be used herein to determine magnified eccentricities at midheight.

$\delta_{nsx} e_y = e_y / (1 - P/P_{cx}) = 1.21 / (1 - 94.3/926) = 1.35$ in. (34.3 mm) for which Table A1 gives $P_{nx} = 187$ kips (831.8 kN).

$\delta_{nsy} e_x = e_x / (1 - P/P_{cy}) = 1.03 / (1 - 94.3/267) = 1.59$ in. (40.4 mm) for which Table A1 gives $P_{ny} = 131.5$ kips (584.9 kN).

$P_{n0} = 266.5$ kips (1185.4 kN), and Eq. (2) $1/P_{nx} + 1/P_{ny} - 1/P_{n0} = 1/P_{ni}$ gives $1/187 + 1/131.5 - 1/266.5 = 1/108.7$ or the value of $P_{ni} = 108.7$ kips (483.5 kN) is greater than the value for which moment magnifiers are determined. Try $P_{ni} = 104.7$ kips (465.7 kN), and repeat the analysis.

$\delta_{nsx} e_y = e_y / (1 - P/P_{cx}) = 1.21 / (1 - 104.7/926) = 1.36$ in. (34.5 mm) for which Table A1 gives $P_{nx} = 186.5$ kips (829.6 kN).

$\delta_{nsy} e_x = e_x / (1 - P/P_{cy}) = 1.03 / (1 - 104.7/267) = 1.59$ in. (40.4 mm) for which Table A1 gives $P_{ny} = 126.0$ kips (560.4 kN).

$P_{n0} = 266.5$ kips (1185.4 kN), and Eq. (2) $1/P_{nx} + 1/P_{ny} - 1/P_{n0} = 1/P_{ni}$ gives $1/186.5 + 1/126.0 - 1/266.5 = 1/104.7$. Because the value of P_{ni} is the same as the value used for moment magnification, 104.7 kips (465.7 kN) is the failure load.

Method 3—Eq. (3): The Australian Standard

The Australian Standard gives Eq. (3) for the exponent α to be used in Eq. (1a) as

Table A1—Demonstration specimen—failure loads P_n (kN) for various eccentricities (mm)

Eccentricity	0	12.7	25.4	38.1	50.8	63.5	76.2	88.9	101.6	P_{nb}
Bent about major axis	1185.4	1043.1	914.1	797.5	696.1	608.5	533.8	471.5	273.1	373.6
Bent about minor axis	1185.4	960.3	765.9	607.2	483.9	391.9	323.8	273.1	226.8	269.1

$$1 \leq \alpha = 0.7 + (1.7P_{ui})/(0.6P_{n0}) \leq 2$$

An iterative procedure must be employed because the strength P_{ui} is a factor in the formulation of the value α as well as for moment magnifiers from slenderness effects. The reported failure load $P_{ni} = 94.3$ kips (419.4 kN) and $\phi = 0.7$ were selected as a trial value. The section strength given in Table A1 continues to apply.

$P_{ui}/P_{n0} = (0.7)94.3/266.5 = 0.2476$. Because this value is > 0.106 and < 0.459 , $\alpha = 0.7 + [(1.7)(0.7)94.3]/[(0.6)266] = 1.4$.

For $P_{ni} = 94.3$ kips (419.4 kN), moment magnification factors from Method 1 indicated that $M_{nx} = 127.0$ kip-in. (14.4 kN-m) and $M_{ny} = 150.2$ kip-in. (17.0 kN-m). Table A1 with $P_{ni} = 94.3$ kips (419.4 kN) indicates that $M_{x0} = 376.3$ kip-in. (42.5 kN-m) and $M_{y0} = 221.6$ kip-in. (25.0 kN-m). With these values and $\alpha = 1.4$, Eq. (1) gives $(127.0/376.3)^{1.4} + (150.2/221.6)^{1.4} = 0.80$. Because Eq. (1a) has a value less than 1, the section will not fail, and a larger load P_{ni} can be tried.

Let $P_{ni} = 110.4$ kips (491.1 kN). Then $\alpha = 0.7 + [(1.7)(0.7)110.4]/[(0.6)266.5] = 1.5216$.

Magnified end moments calculated as before become:

$\delta_{nsx}M_{nx} = P_{ni}e_y/(1 - P/P_{cx}) = 110.4(1.21)/(1 - 110.4/926) = 151.7$ kip-in. (17.1 kN-m); and $\delta_{nsy}M_{ny} = P_{ni}e_x/(1 - P/P_{cy}) = 110.4(1.03)/(1 - 110.4/267) = 193.9$ kip-in. (21.9 kN-m)

Table A-1 indicates for $P_{ni} = 110.4$ kips (491.1 kN), $M_{x0} = 369$ kip-in. (41.7 kN-m) and $M_{y0} = 217$ kip-in. (24.5 kN).

With these values and $\alpha = 1.5216$, Eq. (1) gives $(151.7/369)^{1.5216} + (193.9/217)^{1.5216} = 1.10$, indicating that the failure load is less than 110.4 kips (491.1 kN). Thus, the failure load is estimated to be 105 kips (467.0 kN).

Method 4—Eq. (4): The equation of failure surface

Slenderness effects from the magnitude of axial force P_{ni} make the analysis process an iterative exercise as demonstrated for the other three methodologies. Let the first trial value of P_{ni} be taken as $P_{ni} = 98.3$ kips (437.2 kN) in this application of Eq. (4) to the 5th Furlong's test specimen. Magnified end moments become:

$\delta_{nsx}M_{nx} = P_{ni}e_y/(1 - P/P_{cx}) = 98.3(1.21)/(1 - 98.3/926) = 133.0$ kip-in. (15.0 kN-m); and $\delta_{nsy}M_{ny} = P_{ni}e_x/(1 - P/P_{cy}) = 98.3(1.03)/(1 - 98.3/267) = 160.2$ kip-in. (18.1 kN-m).

For $P_{ni} = 98.3$ kips (437.2 kN), Table A1 gives eccentricities for which $M_{nbx} = 3.58(98.3) = 352$ kip-in. (39.8 kN-m) and $M_{nby} = 2.25(98.3) = 221.5$ kip-in. (25.0 kN-m). The critical section is at midheight of the specimen where the angle of skew can be taken as the arctan $(\delta_{nsx}M_{nx}/\delta_{nsy}M_{ny}) = \arctan(133.0/160.2) = 39.7$ degrees away from the Y (weak) axis. Linear interpolation between values of P_{nbx} and P_{nby} from Table A-1 to establish P_{nb} as $P_{nby} + (39.7/90)(P_{nbx} - P_{nby}) = 60.5 + (39.7/90)(84.0 - 60.5) = 70.9$ kips (315.4 kN).

Equation (4) gives: $(P_{ni} - P_{nb})/(P_{n0} - P_{nb}) + (M_{nx}/M_{nbx})^{1.5} + (M_{ny}/M_{nby})^{1.5} = (98.3 - 70.9)/(266.5 - 70.9) + (133.0/352)^{1.5} + (160.2/221.5)^{1.5} = 0.998$, a value very close to 1. The Method 4 analysis indicates that the failure load is slightly more than 98.3 kips (437.2 kN).

APPENDIX B

Sample examples

Given the usual design condition for which proportions for width b and depth h are known, required values are known for load P_u and moments M_{ux} and M_{uy} , and material strengths f'_c and f_y are known, the following design procedure is recommended.

1. Compute a resultant moment for design $M_{ui} = 1.1 \sqrt{M_{ux}^2 + (M_{uy}h/b)^2}$;
2. Select a section for P_{ui} with M_{ui} acting about the major axis. Distribute reinforcement about the perimeter of the section; and

3. Check the section according to the reciprocal load equation using P_{ux} as the load capacity for an eccentricity $e_y = M_{ux}/P_{ui}$ and using P_{uy} as the capacity for an eccentricity $e_x = M_{uy}/P_{ui}$.

If slenderness must be considered, the required moments M_{ux} and M_{uy} at the end should be increased somewhat before sections are sized with the steps recommended. After the trial section is known, required magnified moments $\delta_{nsx}M_{ux}$ and $\delta_{nsy}M_{uy}$ can be determined.

Design Example 1—Using $f'_c = 5$ ksi (34.5 MPa) and Grade 60 steel, select a square section for a column to support $P_u = 430$ kips (1912.6 kN), $M_{ux} = 128$ kip-ft (173.6 kN-m), and $M_{uy} = 100$ kip-ft (135.6 kN-m). Design tables from References 12 and 13 will be used.

1. Compute $M_{ui} = 1.1 \sqrt{M_{ux}^2 + (M_{uy}h/b)^2} = 179$ kip-ft (242.7 kN-m);
2. With $e_x = M_{ui}/P_{ui} = 179(12)/430 = 5.00$ in. (127 mm), try a 16 in. (406.4 mm) square column with eight No. 8 bars; and
3. For the selected section, $P_{u0} = 1007$ kips (4479 kN), with $e_y = M_{ux}/P_{ui} = 3.57$ in. (90.7 mm); $P_{ux} = 579$ kips (2575.4 kN); $e_x = M_{uy}/P_{ui} = 2.79$ in. (70.9 mm), $P_{uy} = 654$ kips (2909.0 kN).

Equation (2) gives $1/P_{ui} = 1/P_{ux} + 1/P_{uy} - 1/P_{u0} = 1/579 + 1/654 - 1/1007 = 1/442$.

Because calculated $P_{ui} = 442$ kips (1966.1 kN) $>$ required $P_u = 430$ kips (1912.6 kN), the section is satisfactory.

Design Example 2—Select Grade 60 reinforcement needed for a section 16 in. (406.4 mm) wide and 20 in. (508.0 mm) thick to support an axial load of 827 kips (3678.5 kN) when $M_{ux} = 140$ kip-ft (189.8 kN-m) and $M_{uy} = 165$ kip-ft (223.7 kN-m) with $f'_c = 5.0$ ksi (34.5 MPa). The moment M_{uy} acts about the weak axis of the section.

1. Compute $M_{ui} = 1.1 \sqrt{M_{ux}^2 + (M_{uy}h/b)^2} = 274$ kip-ft (371.5 kN-m);
2. With $e_x = M_{ui}/P_{ui} = 274(12)/827 = 3.98$ in. (101.1 mm), try 10 No. 10, 4 on long face, 3 on short face; and
3. For the selected section, $P_{u0} = 1448$ kips (6440.7 kN), with $e_y = M_{ux}/P_{ui} = 2.03$ in. (51.6 mm); $P_{ux} = 1121$ kips (4986.2 kN); $e_x = M_{uy}/P_{ui} = 2.39$ in. (60.7 mm); and $P_{uy} = 1000$ kips (4448.0 kN).

Equation (2) gives $1/P_{ui} = 1/P_{ux} + 1/P_{uy} - 1/P_{u0} = 1/1121 + 1/1000 - 1/1448 = 1/832$.

Because calculated $P_{ui} = 832$ kips (3700.7 kN) $>$ $P_u = 827$ kips (3678.5 kN), the reinforcement is satisfactory.